Jurnal Teknologi

Full Paper

DETERMINATION OF PETROPHYSICAL PROPERTIES CUTOFF IN HETEROLITHIC RESERVOIRS IN MALAY BASIN

Stanley Jaul Kampit[a]*, Samira Albati Kamaruddin[b], Akhmal Sidek[c], Rodziah Rejab[a], Zulkarnain Abdullah Anas[a], Mohd Nor Hisham Mohd Azam[d]

[a]KUFPEC Malaysia, Level 33 Menara Permata Sapura, KLCC, 50088 Kuala Lumpur, Malaysia
[b]Department of Engineering and Technology Razak Faculty of Technology and Informatics Universiti Teknologi Malaysia, 54100 Kuala Lumpur, Malaysia
[c]Petroleum Engineering Department, School of Chemical and Energy Engineering, Faculty of Engineering, Universiti Teknologi Malaysia, 81310 UTM Johor Bahru, Johor Malaysia
[d]Petrofac Malaysia Ltd, Level 28, Menara Prestige 1 Jalan Pinang 50450 Kuala Lumpur, Malaysia

Article history
Received
15 June 2022
Received in revised form
8 November 2022
Accepted
15 November 2022
Published Online
23 February 2023

*Corresponding author
skampit@kufpec.com

Graphical abstract

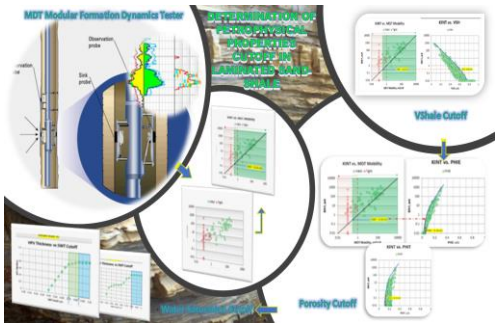

Abstract

Thinly bedded sand-shale heterolithic are commonly found as a marginal reservoir in the Malay Basin. In the evaluation of heterolithic reservoirs, a key challenge is to determine the appropriate petrophysical properties cutoff. This study used the Modular Dynamic Tester (MDT) pressure tests to determine the appropriate petrophysical properties cutoff applicable to heterolithic intervals. Intrinsic permeability analysis and MDT mobility plots were used to determine the cutoffs for shale volume and total porosity. Subsequently, hydrocarbon pore volume thickness (with shale volume and porosity cutoff applied) was plotted against water saturation to determine the water saturation cut-off value. In this case study, the reservoir cutoffs applied are shale volume less than 60% and total porosity in excess of 12%. The hydrocarbon pay cutoff was set at a water saturation less than 85%.

Keywords: MDT pressure test, reservoir characterization, petrophysical cutoff, formation evaluation, heterolithic sand

Abstrak

Heterolitik pasir berlapis nipis biasanya ditemui sebagai takungan marginal di Malay Basin. Dalam penilaian takungan heterolitik, cabaran utama adalah untuk menentukan *cutoff* sifat petrofizik yang sesuai. Kajian ini menggunakan ujian tekanan Modular Dynamic Tester (MDT) untuk menentukan *cutoff* sifat petrofizik yang sesuai untuk lapisan heterolitik. Analisis kebolehtelapan intrinsik dan plot mobiliti MDT digunakan untuk menentukan *cutoff* bagi isipadu syal dan jumlah keliangan. Selepas itu, ketebalan isipadu liang hidrokarbon (dengan isipadu syal dan *cutoff* keliangan digunakan) telah diplot terhadap ketepuan air untuk menentukan nilai potong ketepuan air. Dalam kajian ini, *cutoff* takungan yang digunakan ialah isipadu syal kurang Dari pada 60%, dan jumlah

keliangan melebihi 12%. Hidrokarbon *pay cutoff* ditetapkan pada ketepuan air kurang daripada 85%.

Kata kunci: Ujian tekanan MDT, pencirian takungan, *cutoff* petrofizik, penilaian formasi, pasir heterolitik

1.0 INTRODUCTION

The Malay Basin is located offshore east of Peninsular Malaysia and is the most prolific oil and gas-producing basin in Malaysia [1, 2, 3]. Heterolithic thinly bedded intercalations of sand and shale are a common reservoir type in the Malay Basin. The depositional environment controls the petrophysical properties of heterolithic reservoirs [4, 5, 6, 7, 8], especially the reservoir quality indicators such as shale volume, porosity, permeability, and water saturation [3, 9, 10]. Sand and shale rock type are incorporated within the sediments during or shortly after deposition [10, 11]. The heterolithic reservoir quality is partly controlled by grain size and clay or shale content with the thinly bedded sand shale interval and diagenesis during the sedimentation process [5, 8].

The thinly bedded sand shale from centimetres (cm) to millimetres (mm) scale will affect the heterolithic reservoir permeability and fluid mobility in vertical and horizontal directions. Whilst vertical permeability is nearly zero in most cases, horizontal permeability of heterolithic reservoirs can be sufficient to create an effective petroleum system [10, 12, 13, 14]. The pore space in the sand laminae can store significant volumes of movable hydrocarbons [1, 13].

In most oil or gas field developments, heterolithic reservoirs are considered minor reservoirs and secondary targets to be developed as an upside to the primary conventional reservoirs targets [15]. Petrophysical evaluation of thinly bedded and laminated sandstone-shale intervals is challenging due to the insufficient vertical resolution of logging tools. Log readings of the sandstone laminae are commonly suppressed by shoulder effects [16] and sometimes are not resolved at all [17, 18]. Vertical and lateral compartmentalisation due to stratigraphic complexities or small faults is common [19]. Finally, heterolithic sandstone reservoirs usually suffer from relatively low recovery factors, less than 30% [20].

This study proposes to determine the heterolithic reservoir's petrophysical properties cutoff using the MDT pressure point from exploration, appraisal wells, and infill drilling and used to calculate the pressure gradients, allowing the reservoir's true static and dynamic behaviours to be identified [21].

Grayson S.T. 2000, used MDT to determine the reservoir pressure, fluid identification, and formation permeability [22]. The MDT data is successfully used to determine reservoir permeability and the reliability of electrical image logs for the calculation of reservoir parameters [23, 24]. Haldia *et al*., 2013, used MDT pressure data with a CMR log to determine the reservoir properties [25]. The MDT test data with the existing core test was used by Wei Xu *et al*, 2018 [26] to determine the net reservoir cutoffs. The average permeability estimated from MDT pressure transient analysis was successfully used to determine the net pay cut-off in the Abadi field [27]. Integrating MDT, NMR logs, and conventional logs provide formation permeability and the heterogeneity of the reservoir, as mentioned by Tangyan, L. *et al*. 2005 [28]. The MDT data was also used for the calibration of pore pressure estimation using seismic inversion. [29]

Detailed field data studies include cores data, field analogue, logs, image logs, and other geological data to evaluate the reservoir properties and identify the different lithofacies [30]. The aim is to determine and precisely identify the cutoff value to be applied deterministically at thinly bedded sand shale intervals to classify the reservoir properties that contribute to the estimation of hydrocarbon volume and reservoir mobility and directly indicate the reservoir potential.

Determining the formation of petrophysical properties cutoff faces many challenges with significant uncertainties and impacts on the formation evaluation result. The formation property cutoff is applied to analyse various reservoir properties in the conventional interpretation. The four primary reservoir properties involved in the cutoff determination study are shale volume, porosity, permeability, and water saturation. The challenges and uncertainties in determining the reservoir properties cutoff include formation thickness uncertainty, especially in laminated reservoir units. The high uncertainty in determining the petrophysical properties cutoff in laminated thin sand shale layers reservoir with millimetres (mm) to centimetres (cm) scale [31]. Estimating pay thickness and hydrocarbon pore volume (HPV) thickness contributed by other petrophysical parameters will significantly impact hydrocarbon volume potential. The core photo and image log in Figure 1 exhibit laminated sand-shale

textures of the studied interval as opposed to dispersed shaly sand.

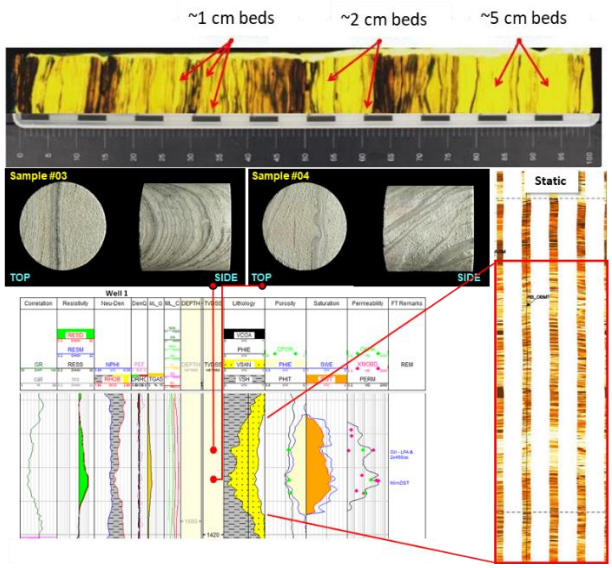

Figure 1 The core photo and image log exhibit laminated sand-shale textures of the studied intervals. The thin bed thickness is below the vertical resolution of standard mode log measurements of 12 – 36 inches (~ 30 – 90 cm)

2.0 DATA AND METHODS

2.1 Data

The dataset for the study comprises both regional and specific data of selected wells, analyses and reports covering most geological aspects, including information up to the most recent seismic and appraisal campaigns in 2013, 2014 and 2021. A total of nine wells was used in the studies, and the acquired data consists of the conventional open hole logs (gamma-ray, density, neutron, and resistivity), sonic logs (compressional and shear), wells with wellbore images (WBI), six wells with formation tests (MDT and DST) and one well with conventional core data. The overview of the studied field shows in Figure 2. The conventional logs covered the E to H groups (Figure 3). The full-bore conventional core is available from the Lower H group, and four wells with a total of 11 sidewall cores are from studies intervals.

The well log data, in general, is of good quality; the borehole is on gauge, where the caliper reading is similar to the bit size reading. There are many vintage wells drilled with water and oil-based mud. Modern logs, such as NMR and wellbore images, are available from six wells. This data helps in providing an additional means of assessing the property and geometry of the formation. Although not all information was available when the analysis was performed, these sidewall cores should provide lithology, formation geometry, porosity, and permeability information. Wellbore images are also available, providing continuous insights into the formation geometry for the geological events larger than the tool's vertical resolution.

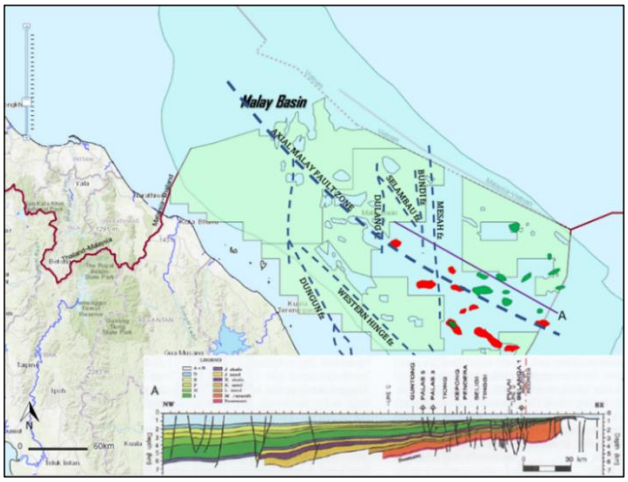

Figure 2 Malay Basin outline. (A) Map of oil and gas fields in the southern part of the Malay Basin, showing the major oil/gas trends. (B) NW-SE cross-section of Malay Basin indicated the sediment thickness, Modified from EPIC-1994, Madon *et al*., 2006; IHS, 2022 [32, 33, 34]

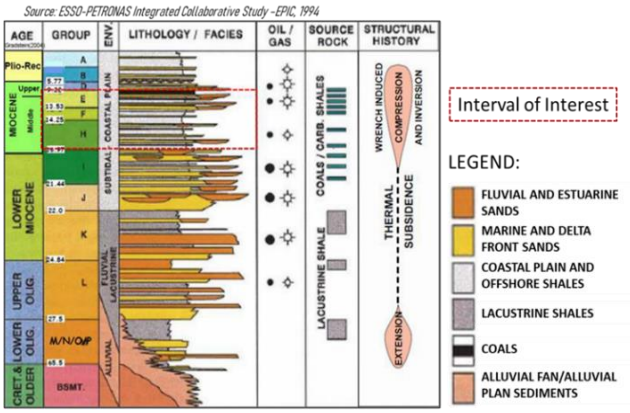

Figure 3 Generalized stratigraphy of the reservoir basin. The samples in this study were extracted from the Middle Miocene, where most of the hydrocarbons are produced [35]

The stratigraphic of the Malay Basin is directly related to structural evaluation, which started from the Synrift phase in the early pre-Miocene [35]. The tectonic thermal subsidence of the Malay Basin started in the early to middle Miocene, when basin inversion happened. The studied interval was deposited in the marine-dominated environment to deltaic sediments with fluvial estuarine channels. The abundance of coal-bearing strata in the studied intervals indicates the possible subtidal to the coastal plain environment.

2.2 Methods

The thin-bedded analysis method utilizes available core and high-resolution resistivity-based wellbore images together with open-hole logs. These are used as inputs to generate a set of petrophysical properties via a log resolution enhancement (LRE) as described by Chong [16], which is more representative of the study intervals. The dataset from the studied field provides the MDT pretest mobility data, which is plotted against the intrinsic permeability (KINT) data to generate the distribution that segregates the valid and tight points (Figure 4). The KINT permeability is a permeability correlation developed by Mike Herron (Schlumberger), and it is a function of a volume of shale (VSH) and porosity [36]. The inputs for calculating the KINT are from porosity and shale volume (VSH) logs. The VSH log is calculated by using GR and NPHI-RHOB. The Porosity log is generated from RHOB. The result of the KINT log is compared and matched to NMR permeability and core data for calibration and to ensure a realistic result. Similarly, the log-estimated porosity compared to core data porosity.

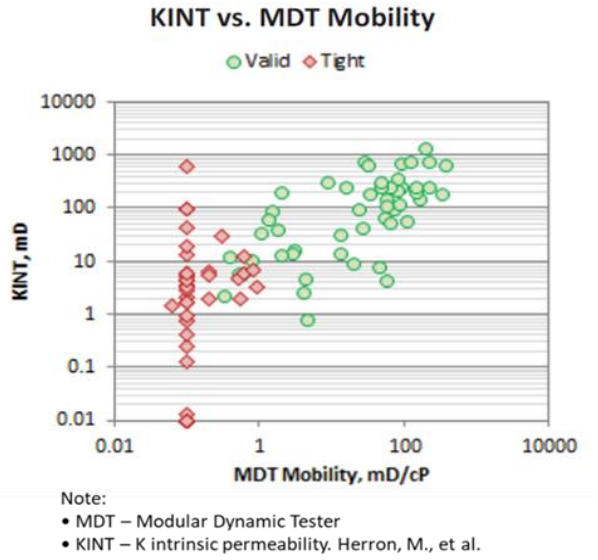

Figure 4 MDT versus intrinsic permeability (KINT) data distribution plot

The MDT data is an input to determine the petrophysical properties in this study. The MDT data used are valid points and verified by the vendor or tools operator. The tools limit is around 0.1 mD/cp, and the tight points might be much smaller. The overlapping tight and good points are anticipated due to the point sample taken at the heterolithic intervals. Four primary properties cutoff determine using this method are namely shale volume (VSH), permeability (K), porosity (Ø), and water saturation (SWT). The first step is to determine the intrinsic permeability (KINT) cutoff using MDT pretest mobility data as a primary input.

1. Calculate the KINT permeability log from total porosity and shale-bound water Derive the KINT values for each of the MDT mobility data points.
2. Plot the KINT permeability versus MDT mobility data
3. Successful MDT pretest (valid) and unsuccessful (tight) points are segregated from the plot.
4. The corresponding KINT cutoff determined above data points where the formation can contribute to the reservoir flow and vice versa.

The volume of shale is estimated mainly from density and neutron logs; GR logs have also been used over the zones where density or neutron logs are believed to be affected by hole enlargements or washout effects.

The determination of shale volume (VSH) and porosity (Ø) cutoff are using the intrinsic permeability (KINT) cutoff as a proxy. The several steps below are applied.

1. Derive the VSH log using GR and neutron density (NPHI-RHOB) logs.
2. The total porosity is estimated from a density log with a matrix density of 2.65 g/cc and fluid density of 0.80 g/cc; the effective porosity is estimated by subtracting shale-bound water from the total porosity, where the shale total porosity value used is 0.10 v/v.
3. Intrinsic permeability (KINT) data plotted against shale volume or porosity data.
4. Establish the relationship between intrinsic permeability and shale volume or porosity from the data plot.
5. Using determine intrinsic permeability (KINT) cutoff as a proxy, the corresponding shale volume (VSH) and porosity cutoff are determined.

The water saturation derives using the Leverett-J saturation function (SHF_LJ). The SHF_LJ is derived based on the available core centrifuge capillary pressure data using the normalized capillary pressure. The Total Water saturation (SWT) cutoff for studied intervals is determined using the hydrocarbon pore volume (HPV) thickness data as the primary input. The HPV thickness results from the shale volume estimation and porosity parameter determined from the cutoff applied. The workflow involves several steps as below:

1. Derive the hydrocarbon pore volume (HPV) thickness sensitivities using free define SWT cutoff.
2. The HPV thickness result of the free defined SWT cutoff is plotted in the sensitivity graph.
3. The sensitivity of the HPV thickness to the SWT cutoff values is analyzed from the HPV thickness versus SWT cutoff values plot.

4. The SWT cutoff values for the interested reservoir are determined from the plot when the HPV thickness is no longer sensitive to the SWT cutoff values.

The flow chart represents all processes involved in the research work, as shown in Figure 5.

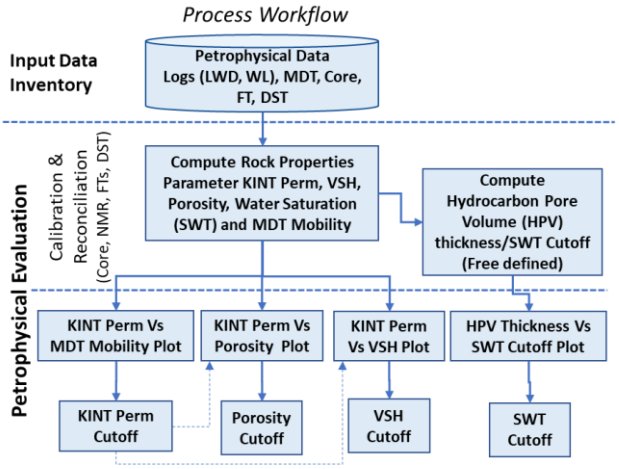

Figure 5 Flowchart illustrates the work processes involved in determining the petrophysical cutoff in the heterolithic intervals.

3.0 RESULTS

3.1 Intrinsic Permeability Cutoff

On the plot of intrinsic permeability (KINT) against MDT mobility, there is an overlap between valid and tight points. In Figure 6, this domain of overlap where there is uncertainty about the ability of the reservoir to flow is indicated by two vertical lines (dashed). The viscosity fluid that flows into the MDT tool could be affected by drilling mud and formation fluid, as most of the MDT points are plotted above the linear relationship line as applied for studied intervals. The mud and the fluid viscosity need to be incorporated into MDT mobility. The KINT cutoff uncertainties applied for the non-linear relationship.

The intersection between the linear relationship line between the MDT mobility and KINT with vertical lines signifies a cutoff point at which the formation responded to the test and is more likely to contribute to the flow and vice versa. The intersection point translates to the KINT value cutoff in this study which considers a minimum cutoff value equivalence to 0.3 mD. The KINT value of 1.0 mD cutoff will exclude the thinly bedded sand as the reservoir potential with the heterolithic reservoir interval.

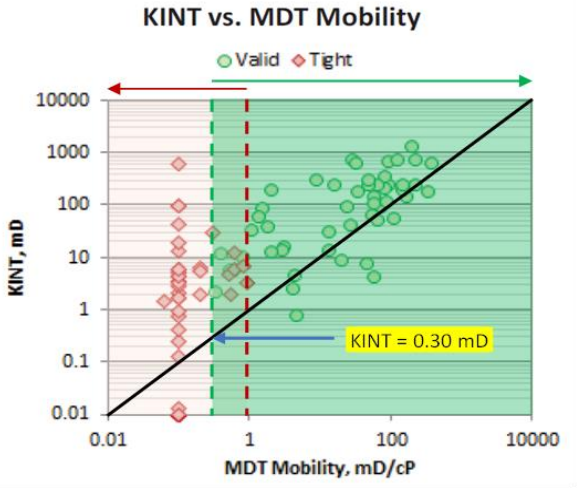

Figure 6 The intrinsic permeability (KINT) and MDT data plot. Vertical lines (dashed) represent the minimum valid point and the maximum tight point

3.2 Shale Volume (VSH) Cutoff

The shale volume cutoff value determination using the 0.3 mD of permeability cutoff. The shale volume (VSH) data are plotted against the KINT data to generate the data transform distribution between those datasets. The relationship between the KINT data and the VSH is established; in this case, the relationship is chosen as the maximum boundary from the KINT-VSH distribution. Based on the selected minimum KINT cutoff value of 0.3 mD, the corresponding VSH value from the distribution plot will be 0.6 v/v or 60% of shale volume, as shown in Figure 7. The 60% shale volume is the equivalent cutoff applied for the interested reservoir.

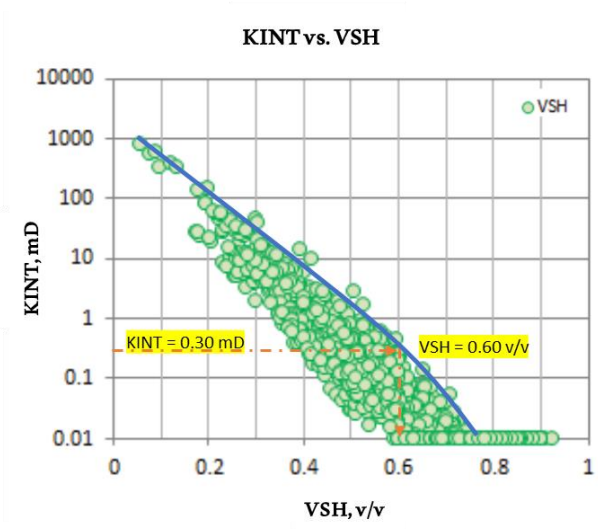

Figure 7 The KINT permeability versus MDT mobility (mD/cP) and shale volume (VSH) plots were used to determine the VSH cutoff

3.3 Porosity Cutoff

The porosity cutoff value determination was applied for both total porosity and effective porosity. Both parameters are essential to determining the reservoir quality and other parameters contributing to the hydrocarbon volume estimation. To determine the total porosity (Øt) and the effective porosity (Øe), the KINT permeability data is plotted against the porosity data. Both total and effective porosity data distribution plots were created separately to independently distinguish their relationship with KINT permeability.

The boundary line was generated to determine the minimum porosity data relationship from the distribution data plot. From the total porosity (Øt) versus KINT permeability plot (Figure 8), the corresponding Øt value is 0.12 v/v or 12% when the KINT permeability is equal to 0.3 mD as the determined cutoff. Therefore, the total porosity cutoff value of 12% was applied to classify the flow reservoir unit in this study field. The effective porosity cutoff value determines by effective porosity (Øe) versus the KINT permeability plot (Figure 9). From the plot, the corresponding Øe value is 0.05 v/v or 5% when the KINT permeability is equal to 0.3 mD. Therefore, the reservoir quality contributing to the flow unit is defined as ≥5% of the effective porosity value.

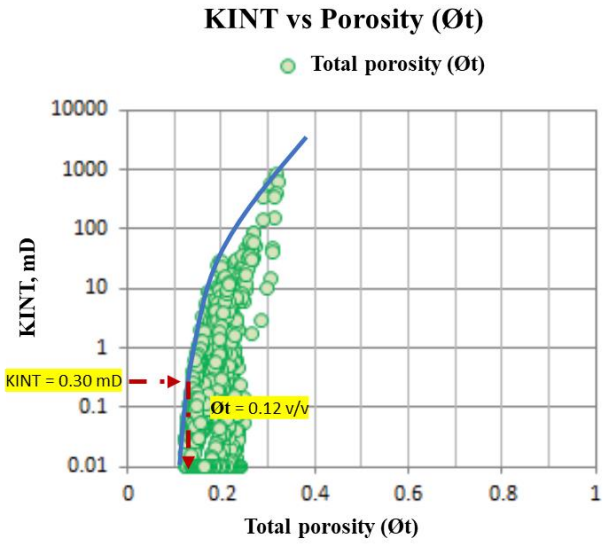

Figure 8 The KINT permeability versus MDT mobility (mD/cP) and Total porosity (Øt) plots were used to determine the total porosity (Øt) cutoff

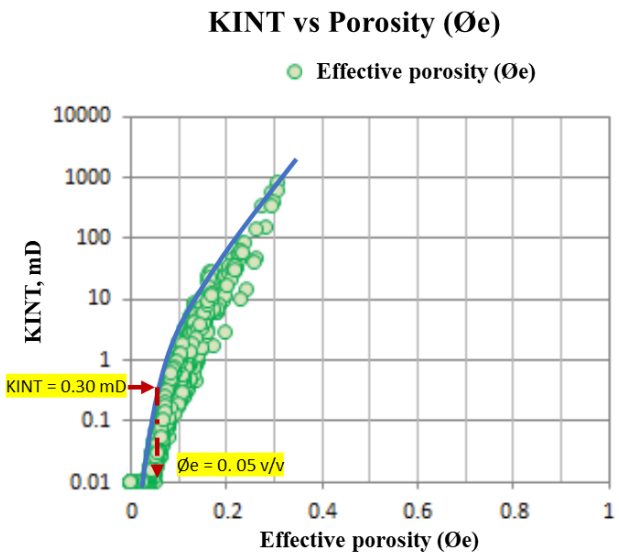

Figure 9 The KINT permeability versus MDT mobility (mD/cP) and effective porosity (Øe) plots were used to determine the effective porosity (Øe) cutoff

3.4 Water Saturation Cutoff

The water saturation cutoff determination is not directly based on the MDT and KINT permeability relationship. The Leverett-J saturation function was used to derive the water saturation at studied intervals. The saturation high function is derived based on core centrifuge capillary pressure data using the normalized wetting phase at capillary pressure data.

However, the estimation of hydrocarbon pore volume (HPV) thickness results from a direct calculation from VSH used to determine the net sand volume and porosity. The net sand property is obtained by applying the 60% cutoff on the VSH. An additional cutoff is also applied to obtain property summary sets for net sand with total porosity values equal to and above 0.12 v/v.

The result of HPV thickness data is plotted against the SWT analysis of cutoff values to generate the distribution plot, as shown in Figure 10. These SWT cutoff values were combined with the VSH and porosity cutoffs to obtain the HPV thickness at the reservoir level of the reservoir of interest. The reservoir SWT cutoff value is set at the point beyond which HPV thickness is no longer sensitive to the SWT cutoff value. As indicated in Figure 11, there are differences between individual reservoirs. In Reservoir A, whilst there is no hydrocarbon in rock with SWT more than 85%, virtually all of the hydrocarbon is in fact stored in rock with less than 70% SWT cutoff value may provide a more realistic estimation. The HPV thickness versus SWT cutoff plot for reservoir B provides a clearer cutoff at an 80% SWT value.

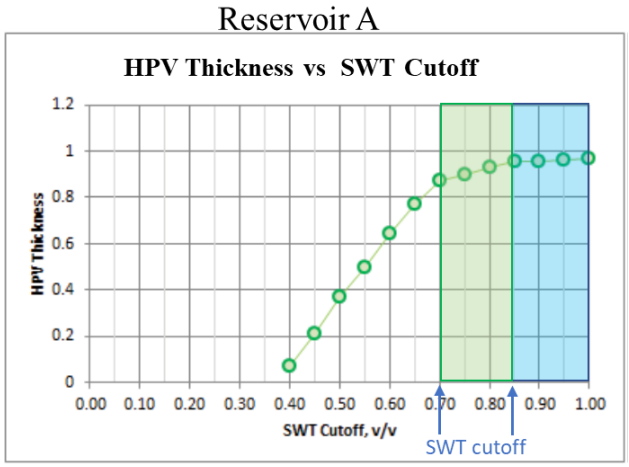

Figure 10 The data from Reservoir A - HPV Thickness versus SWT cutoff, v/v plots. The SWT cutoff ≤85% is determined by HPV thickness sensitivity

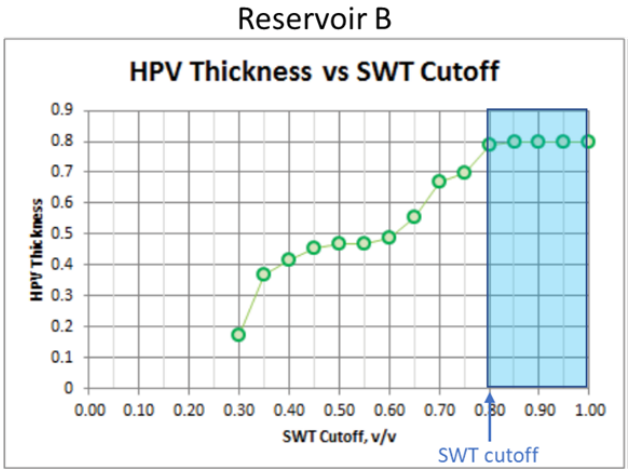

Figure 11 The data from Reservoir B - HPV Thickness versus SWT cutoff, v/v plots. The SWT cutoff ≤80% is determined by HPV thickness sensitivity

4.0 DISCUSSION

The result from thin bed analysis applied at heterolithic reservoir intervals improves the pay thickness, permeability and saturation estimations. For net pay thickness, the improvement is attributed to the removal of shoulder bed effects, re-inclusion of sand laminations in pay summation and the removal of shale laminations from thick reservoirs, as described by Chong [16]. For saturation, clay laminations are correctly accounted for in the Dual Water Model or Waxman Smits equations. Porosity and VSH provide more realistic inputs to the permeability transform.

The study provides realistic results for the petrophysical properties cutoff determination using the MDT pretest pressure data to evaluate the potential of a heterolithic reservoir by including the laminated thinly bedded sand from thin bed analysis results. The KINT permeability cutoff value of 0.3 mD is the minimum mobility recorded from valid MDT data points obtained from the field and is more likely to be able to contribute to the formation flow. The lower limit of effective and total porosity cutoff is between 5% and 12%. This will create uncertainty in reservoir quality which will obviously impact on hydrocarbon in place and reserves estimation [37]. The result shows that the laminated thinly bedded sand is included in the HPV thickness analysis from heterolithic reservoir intervals. The porosity cutoff affected the values of the corresponding VSH and SWT cutoffs [38] and the KINT permeability from other fields may have a different cutoff based on the MDT data obtained from that particular field and reservoirs.

However, the same methodology can be applied to determine the property cutoff as the approach uses the actual field data recorded. The realistically applied SWT cutoff value improves the estimation of HPV thickness to include the thinly bedded sand. These results prove that the applied properties cutoff provides a realistic outcome in a reservoir definition as a result tabulated in Table 1, which significantly impacts the volume estimation process.

Table 1 The heterolithic reservoir interval properties summary using a defined cutoff from the MDT method

Well	Interval	TOP mTVDSS	BASE mTVDSS	NET mTVD	NTG m/m	KH mD.m	Øt v/v	SWT v/v	VSH v/v	K mD
W1	HL	1403.0	1428.8	18.6	0.72	225.3	0.20	0.52	0.30	12.1
W2	HL	1387.1	1408.3	11.1	0.53	64.9	0.19	0.61	0.39	5.8
W3	HL	1393.6	1419.3	18.4	0.72	290.8	0.20	0.50	0.35	15.8
W4	HL	1360.1	1380.9	9.4	0.45	165.8	0.20	0.58	0.40	17.6
W5	HL	1426.6	1456.5	20.0	0.67	228.5	0.19	0.56	0.35	11.4
W6	HL	1382.3	1402.2	6.4	0.32	41.9	0.19	0.63	0.37	6.5
W7	HL	1448.9	1479.0	19.9	0.66	62.2	0.17	0.72	0.38	3.1
W8	HL	1450.1	1479.1	18.2	0.63	72.4	0.17	0.69	0.39	4.0
W9	HL	1407.7	1440.3	23.1	0.71	873.7	0.20	0.55	0.32	37.9

VSH ≤ 60%, Øt ≥ 12% and SWT ≤ 85%

5.0 CONCLUSION

The present study deals with petrophysical evaluation to determine the properties cutoff as part of the field hydrocarbon volumetric evaluation. The MDT from the studied field provides the KINT permeability cutoff value of 0.3 mD to include thinly bedded sand. The VSH cutoff value of 60%, total porosity cutoff of 0.12 v/v, and the realistic SWT cutoff determination of 85% and 80%. The application of these properties determined cutoff as a result of MDT pretest pressure data analysis for heterolithic reservoirs with thinly bedded sand-shale, opens the opportunity for extended development and unlocking of the real potential of heterolithic reservoirs thus, creating opportunities for marginal Field Development for the studied field.

Acknowledgement

The author would like to acknowledge all that has contributed to the making of this publication, directly or indirectly.

References

[1] Kantaatmadja, B., Nurhono, A. A., Bt A Majid, R., B Amdan, A. 2014. Unlock Hydrocarbon Volumetric Potential of LRLC Clastic Reservoirs in Malaysian Basins. *International Petroleum Technology Conference*. OnePetro. DOI: https://doi.org/10.2523/IPTC-18236-MS.

[2] Lee, E. T. H. 2013. Scope for improvement: Malaysia's Oil and Gas Sector. Research for Social Advancement.

[3] Madon, M. 2021. Five Decades of Petroleum Exploration and Discovery in the Malay Basin (1968-2018) and Remaining Potential. *Bulletin of the Geological Society of Malaysia*. 72. DOI: https://doi.org/10.7186/bgsm72202106.

[4] Almoqaddam, R. O., Darwish, M., El-Barkooky, A. N., & Clerk, C., 2018. Sedimentary Facies Analysis of the Upper Bahariya Sandstone Reservoir in East Bahariya C Area, North Western Desert, Egypt. Egyptian *Journal of Petroleum*. 27(4): 1103-1112.

[5] Dowey, P. J., Worden, R. H., Utley, J. and Hodgson, D. M. 2017. Sedimentary Controls on Modern Sand Grain Coat Formation. *Sedimentary Geology*. 353: 46-63. DOI: https://doi.org/10.1016/j.sedgeo.2017.03.001.

[6] Massart, B. Y. G. 2014. Improved Characterisation and Modelling of Heterolithic Tidal Sandstone Reservoirs. Doctoral Dissertation. Imperial College London. 39 -108. DOI: https://doi.org/10.25560/24995.

[7] Morad, S., Al-Ramadan, K., Ketzer, J. M. and De Ros, L. F., 2010. The Impact of Diagenesis on the Heterogeneity of Sandstone Reservoirs: A review of the Role of Depositional Facies and Sequence Stratigraphy. *AAPG Bulletin*. 94(8): 1267-1309. DOI: https://doi.org/10.1306/04211009178.

[8] Saïag, J., Brigaud, B., Portier, É., Desaubliaux, G., Bucherie, A., Miska, S. and Pagel, M. 2016. Sedimentological Control on the Diagenesis and Reservoir Quality of Tidal Sandstones of the Upper Cape Hay Formation (Permian, Bonaparte Basin, Australia). *Marine and Petroleum Geology*. 77: 597-624. DOI: https://doi.org/10.1016/j.marpetgeo.2016.07.002.

[9] Petitpierre, L., Frohlich, S., Bodin, S., Grech, P. V., Lang, S., Vachtman, D., Redfern, J. 2021. Sharp-based Shoreface Sandstones in the Early Carboniferous Sediments of the Awaynat Wanin Area (western Libya). *Journal of African Earth Sciences*. 178: 104168. DOI: https://doi.org/10.1016/j.jafrearsci.2021.104168.

[10] Virolle, M., Brigaud, B., Luby, S., Portier, É., Féniès, H., Bourillot, R., Patrier, P., Beaufort, D., 2019. Influence of Sedimentation and Detrital Clay Grain Coats on Chloritized Sandstone Reservoir Qualities: Insights from Comparisons between Ancient Tidal Heterolithic Sandstones and a Modern Estuarine System. *Marine and Petroleum Geology*. 107: 163-184. DOI: https://doi.org/10.1016/j.marpetgeo.2019.05.010.

[11] Griffiths, J. 2018. Mineralogical and Textural Variation in Modern Estuarine Sands: Implications for Sandstone Reservoir Quality. The University of Liverpool (United Kingdom).

[12] Ezabadi, M. G., Ramli, A. S., Ataei, A. and Othman, T. R., 2015. Challenges in Modeling of High Clay Volume Gas Reservoir with No Water Production. *SPE/IATMI Asia Pacific Oil & Gas Conference and Exhibition*. OnePetro. DOI: https://doi.org/10.2118/176251-MS.

[13] Hasnan, H. K., Sheppard, A., Hassan, M. H. A., Knackstedt, M., and Abdullah, W. H. 2020. Digital Core Analysis: Improved Connectivity and Permeability Characterization of Thin Sandstone Layers in Heterolithic Rocks. *Marine and Petroleum Geology*. 120: 104549. DOI: https://doi.org/10.1016/j.marpetgeo.2020.104549.

[14] Verma, A., Shukla, U. K. 2020. Heterolithic Lower Rewa Sandstone of the Neoproterozoic Rewa Group, Vindhyan Basin, UP, India: An Example of Tidal Point Bar. Precambrian Research. 350: 105932. DOI: https://doi.org/10.1016/j.precamres.2020.105932.

[15] Petronas. Research, Scientific Services, & Petronas. Petroleum Management Unit. 1999. The Petroleum Geology and Resources of Malaysia. Petronas.

[16] Chong, E. E., Azam, M. N., James, P. B., Rae, S. F. and Flew, S. 2017. Application of Thin-bed Analysis in Reservoir Modelling to Unlock Further Development Potential of Thinly-bedded Marginal Reservoirs. *SPE/IATMI Asia Pacific Oil & Gas Conference and Exhibition*. OnePetro. DOI: https://doi.org/10.2118/186425-MS.

[17] Jackson, M. D., Yoshida, S., Muggeridge, A. H., & Johnson, H. D. 2005. Three-dimensional Reservoir Characterization and Flow Simulation of Heterolithic Tidal Sandstones. *AAPG Bulletin*. 89(4): 507-528. DOI: https://doi.org/10.1306/11230404036.

[18] Singh, V., Yemez, I., & Sotomayor, J. 2013. Key Factors Affecting 3D Reservoir Interpretation and Modelling Outcomes: Industry Perspectives. *British Journal of Applied Science & Technology*. 3(3): 376. DOI: https://doi.org/10.9734/BJAST/2014/3089.

[19] Riegel, H., Balsamo, F., Mattioni, L., Tondi, E. 2019. Petrophysical Properties and Microstructural Analysis of Faulted Heterolithic Packages: A Case Study from Miocene Turbidite Successions, Italy. Geofluids, 2019. DOI: https://doi.org/10.1155/2019/9582359.

[20] Martinius, A. W., Ringrose, P. S., Brostrøm, C., Elfenbein, C., Næss, A., and Ringås, J. E. 2005. Reservoir Challenges of Heterolithic Tidal Sandstone Reservoirs in the Halten Terrace, Mid-Norway. *Petroleum Geoscience*. 11(1): 3-16. DOI: https://doi.org/10.1144/1354-079304-629.

[21] Belhouchet, H. E., Benzagouta, M. S., Dobbi, A., Mazouz, E., Achi, N., Duplay, J., and Khodja, M. 2021. Reservoir Compartmentalization and Fluid Property Determination using a Modular Dynamic Tester (MDT): Case Study of an Algerian Oil Field. *Euro-Mediterranean Journal for Environmental Integration*. 6(1): 1-13. DOI: https://doi.org/10.1007/s41207-020-00216-5.

[22] Grayson, S. T., Morris, C. W. and Blume, C. R. 2000. Fluid Identification and Pressure Transient Analysis in the Fractured Monterey Using The Modular Dynamics Tester. *SPE/AAPG Western Regional Meeting*. OnePetro. DOI: https://doi.org/10.2118/62532-MS.

[23] Anderson, B. J., Wilder, J. W., Kurihara, M., White, M. D., Moridis, G. J., Wilson, S. J., Pooladi-Darvish, M., Masuda, Y., Collett, T. S., Hunter, R. B. and Narita, H. 2008. Analysis of Modular Dynamic Formation Test Results from the Mount Elbert 01 Stratigraphic Test Well, Milne Point Unit, North Slope, Alaska. British Columbia, Canada.

[24] Aghli, G., Moussavi-Harami, R. and Mohammadian, R., 2020. Reservoir Heterogeneity and Fracture Parameter Determination using Electrical Image Logs and Petrophysical Data (A Case Study, Carbonate Asmari Formation, Zagros Basin, SW Iran). *Petroleum Science*. 17(1): 51-69. DOI: https://doi.org/10.1007/s12182-019-00413-0.

[25] Haldia, B. S., Singh, S., Bhanja, A. K., Samanta, A. and DEO, P. 2013. A New Approach to Determine T 2 Cutoff Value with Integration of NMR, MDT Pressure Data in TS-V Sand of Charali Field. *10th Biennial International Conference & Exposition*. P013.

[26] Xu, W., Zhang, X., Shang, F., Fang, L., Liu, J. and Yang, X. 2018. An Integrated Quantitative Approach for Determination of Net Reservoir Cutoffs: A Case Study of Q Oil Field, Lake Albert, Uganda. *Journal of African Earth Sciences*. 145: 261-266. DOI: https://doi.org/10.1016/j.jafrearsci.2018.05.007.

[27] Fitrio, D., Oentoe, R. and Nomura, M. 2016. Successful MDT Dual Packer Survey for Cut-off Determination in the Abadi Field: Design, Execution, and Analysis.
[28] Tangyan, L., Zaitian, M., Junxiao, W. and Hongzhi, L. 2005. Integrating MDT, NMR Log and Conventional Logs for One-well Evaluation. *Journal of Petroleum Science and Engineering.* 46(1-2): 73-80.
DOI: https://doi.org/10.1016/j.petrol.2004.09.001.
[29] Esmaeilpour, S. and Ispas, I. 2021. June. Pore Pressure Estimation Using Seismic Inversion and Mdt Data. *55th US Rock Mechanics/Geomechanics Symposium.* OnePetro.
[30] Chen, J. 2013. Lithofacies Classification: From Sedimentologic Analysis to 3D Reservoir Modelling. *International Petroleum Technology Conference*. OnePetro.
DOI: https://doi.org/10.2523/16502-MS.
[31] Qassamipour, M., Khodapanah, E. and Tabatabaei-Nezhad, S. A. 2020. Determination of Cutoffs by Petrophysical Log Data: A New Methodology Applicable to Oil and Gas Reservoirs. *Energy Sources, Part A: Recovery, Utilization, and Environmental Effects*. 1-14.
DOI: https://doi.org/10.1080/15567036.2020.1759733.
[32] EPIC. 1994. Generalised stratigraphy, Hydrocarbon Occurences, and Structural History of the Malay Basin. PETRONAS, 1994. The Petroleum Geology and Resources of Malaysia. 182.
[33] Madon, M., Yang, J. S., Abolins, P., Hassan, R. A., Yakzan, A. M. and Zainal, S. B. 2006. Petroleum Systems of the Northern Malay Basin.
[34] HIS. 2022. https://my.ihs.com/Energy/Products (accessed 7 March 2022).
[35] Madon, M., Peter Abolins, Mohammad Jamaal Hoesni & Mansor Bin Ahmad. 1999. Malay Basin. In: PETRONAS The Petroleum Geology and Resources of Malaysia Chapter 8, 171-217.
[36] Herron, M. M. 1987. Estimating the Intrinsic Permeability of Clastic Sediments from Geochemical Data. *SPWLA 28th Annual Logging Symposium*. OnePetro.
[37] Abbasi, S., Singh, T. N. and Pritchard, T. 2016. Error and Impact of Porosity-permeability Transform in Tight Reservoir. *Journal of Natural Gas Science and Engineering.* 35: 354-361.
DOI: https://doi.org/10.1016/j.jngse.2016.08.055.
[38] Ebong, M. and Onyekonwu, M. 2014. Determination of Cutoffs and Implications in Integrated Reservoir Studies. *SPE Nigeria Annual International Conference and Exhibition.* OnePetro.
DOI: https://doi.org/10.2118/172436-MS.